Polarization dependence of spin excitations in $BaCu_2Si_2O_7$

A. Zheludev*
Solid State Division, Oak Ridge National Laboratory, Oak Ridge, Tennessee 37831-6393

S. Raymond and L.-P. Regnault
CEA-Grenoble DRFMC-SPSMS-MDN, 17 rue des Martyrs, 38054 Grenoble Cedex 9, France

F. H. L. Essler
Physics Department, Brookhaven National Laboratory, Upton, New York 11973-5000

K. Kakurai
Advanced Science Research Center, Japan Atomic Energy Research Institute, Tokai, Ibaraki 319-1195, Japan

T. Masuda† and K. Uchinokura
Department of Advanced Materials Science, The University of Tokyo, Tokyo 113-8656, Japan
(Received 25 October 2002; published 4 April 2003)

The polarization dependence of magnetic excitations in the quasi-one-dimensional antiferromagnet $BaCu_2Si_2O_7$ is studied as a function of momentum and energy transfer. The results of inelastic neutron-scattering measurements are directly compared to semianalytical calculations based on the chain-mean-field approximation and random-phase approximation (RPA). A quantitative agreement between theoretically calculated and experimentally measured dynamic structure factors of transverse spin fluctuations is obtained. In contrast, substantial discrepancies are found for longitudinal polarization. This behavior is attributed to intrinsic limitations of the RPA that ignores correlation effects.

DOI: 10.1103/PhysRevB.67.134406 PACS number(s): 75.10.Jm, 75.30.Ds, 75.30.Fv, 75.50.Ee

I. INTRODUCTION

Excitations in weakly ordered quasi-one-dimensional (quasi-1D) antiferromagnets (AFs) are a topic of considerable current interest in the field of quantum magnetism. Particularly intriguing is the problem of the so-called longitudinal mode (LM), a magnon excitation polarized *parallel* to the direction of the ordered moment. The discovery of a coherent LM in $KCuF_3$ (Refs. 1 and 2) confirmed previous theoretical predictions,[3] based on the chain-mean-field[4] (chain-MF) and random-phase approximation (RPA) theories.[5,3] Currently chain-MF/RPA indeed appears to be the most versatile analytical framework for treating weakly coupled quantum spin chains. However, the $KCuF_3$ experiments also highlighted certain limitations of this approach. In particular, the chain-MF/RPA cannot, by its very definition, account for the experimentally observed finite lifetime (broadening) of the LM.

In a recent short paper[6] we reported polarization-sensitive neutron-scattering measurements of the dynamic spin structure factor in another model quasi-1D antiferromagnet, namely, $BaCu_2Si_2O_7$. This $S=1/2$ system has much weaker interchain interactions and low-temperature ordered moments than $KCuF_3$. Preliminary results indicated that, unlike $KCuF_3$, in $BaCu_2Si_2O_7$ there is no well-defined longitudinal mode. Instead, the longitudinal spectrum is best described as a single broad asymmetric continuum feature. This stark discrepancy in the predictions of the chain-MF/RPA model came as a surprise. Indeed, for the *transverse*-polarized spectrum of $BaCu_2Si_2O_7$, earlier neutron-scattering work confirmed excellent agreement with chain-MF/RPA theory, at least as far as excitation energies were concerned.[7,8] The apparent paradox is not fully resolved to date. This is in part due to the fact that only very limited data are available for longitudinal-polarized excitations. Even for the transverse-polarized spectrum, the existing wealth of high-resolution neutron data could not be *quantitatively* compared to theoretical predictions, for lack of calculations based on the specific geometry of interchain interactions in $BaCu_2Si_2O_7$. The present work addresses both these issues and involves a detailed experimental and theoretical study of the polarization dependence of magnetic excitations in this compound. First, we further exploit the technique of polarization analysis described in Ref. 6 to investigate the wave-vector dependence of longitudinal excitations. We then perform chain-MF/RPA calculations of the dynamic structure factor for the exchange topology and constants of $BaCu_2Si_2O_7$. This enables us to perform a direct *quantitative* comparison between theory and experiment for both energies and *intensities* of the coherent and diffuse components of the dynamic spin-correlation functions.

Magnetic interactions in $BaCu_2Si_2O_7$ have been previously thoroughly studied using bulk methods,[9,10] neutron diffraction,[9,11] and inelastic neutron scattering.[9,12,13,8] The silicate $BaCu_2Si_2O_7$ crystallizes in an orthorhombic structure (space group $Pnma$, $a=6.862$ Å, $b=13.178$ Å, $c=6.897$ Å) with slightly zigzag AF $S=1/2$ chains of Cu^{2+} ions running along the c axis. The in-chain exchange constant is $J=24.1$ meV. Interactions between the chains are much weaker, and the characteristic bandwidth of spin-wave dispersion perpendicular to the chain direction is $\Delta=2.51$ meV. $BaCu_2Si_2O_7$ orders antiferromagnetically at

$T_N = 9.2$ K $= 0.033 J/k_B$ with a zero-T saturation moment of $m_0 = 0.15 \mu_B$ parallel to the crystallographic c axis.

II. EXPERIMENTAL PROCEDURES

In the present study we employed the same basic principle of using a tunable horizontal magnetic field to determine the polarization of magnetic excitations in $BaCu_2Si_2O_7$ with unpolarized neutrons, as described in Ref. 6. However, the new experimental setup included several significant improvements compared to the one used previously. First, we utilized a different horizontal field magnet with a much more open coil construction that allowed almost unrestricted scattering geometries within the horizontal plane. This enabled us to collect the data in a series of conventional constant-Q and constant-E scans, which was not possible in the highly restrictive geometry used before. Second, the larger diameter of the magnet bore made it possible to mount the sample with a high-symmetry reciprocal-space crystallographic (a,c) plane horizontal, rather than having a scattering plane defined by some low-symmetry vectors as in previous studies. Third, the experiments were carried out at the IN22 instrument installed at Institut Laue Langevin in Grenoble, France. This instrument boasts a much higher neutron flux which accelerated the data-collection rate considerably, while reducing statistical errors.

All data were collected using a 14.7-meV fixed-final energy configuration with pyrolitic graphite (PG) (002) reflections employed in the vertical-focusing monochromator and flat analyzer. A PG filter was installed after the sample to eliminate higher-order beam contamination. The supermirror neutron guide provided effective premonochromator beam collimation. Soller collimators with a horizontal acceptance of 60 ft were installed before and after the sample. No dedicated collimation devices were used between analyzer and detector. The measurements were performed at momentum transfers $(0,k,l)$ in the vicinity of the 1D AF zone center $l = 1$, for $k = -1 \ldots 0$. The main advantage of working around $l = 1$ (as opposed to $l = 3$, as in previous studies) is a smaller intensity penalty due to the magnetic form factor of Cu^{2+}, and the negligible small 3D modulation of the dynamic structure factor due to the slightly zigzag structure of the spin chains.[14] The tradeoff is limitations on the energy transfer (up to 12 meV in the present experiment) imposed by kinematic constraints on the scattering geometry.

Each data set was measured for two values of magnetic field applied along the crystallographic c axis, $H_1 = 1.5$ T and $H_2 = 2.2$ T. These field values were chosen to be below and just above a spin-flop transition at $H_c = 2.0$ T, respectively.[10,11] The transition involves a reorientation of the ordered staggered magnetization in the system.[11] As explained in Ref. 6, this leads to a drastic change in the polarization-dependent part of the scattering cross section for unpolarized neutrons. The effect on the scattering intensity from longitudinal (parallel to the ordered moment) and transverse (perpendicular to the ordered moment) spin fluctuations is different, which allows us to separate the two components. In general, the measured intensity can be expanded as

$$I(\mathbf{q},\omega) \propto S^{\perp}(\mathbf{q},\omega)(1+\cos^2\alpha_{\mathbf{q}}) + S^{\parallel}(\mathbf{q},\omega)\sin^2\alpha_{\mathbf{q}} + \mathcal{B}(\mathbf{q},\omega). \quad (1)$$

In this equation $S^{\perp}(\mathbf{q},\omega)$ and $S^{\parallel}(\mathbf{q},\omega)$ are the magnetic dynamic structure factors for transverse and longitudinal polarizations, respectively. The wave-vector-dependent angle $\alpha_{\mathbf{q}}$ is measured between the momentum transfer $\mathbf{q}$ and the direction of the ordered moment. The orientations of the latter were previously determined using neutron diffraction in both the low-field (along the c axis) and in the spin-flop (roughly along a) states, so $\alpha_{\mathbf{q}}$ is a known quantity for every scan measured. The quantity $\mathcal{B}(\mathbf{q},\omega)$ is the polarization-independent background determined separately, as discussed below. In our measurements $S^{\perp}(\mathbf{q},\omega)$ and $S^{\parallel}(\mathbf{q},\omega)$ could thus be extracted from pairs of scans at H_1 and H_2 by solving a set of two coupled linear equations for each point.

For this procedure to work, exact knowledge of $\mathcal{B}(\mathbf{q},\omega)$ is required. $\mathcal{B}(\mathbf{q},\omega)$ includes both intrinsic (coherent and incoherent nuclear scattering in the sample) and extrinsic (scattering in the sample holder, magnet, etc.) contributions. In our previous experiments only the latter part was measured. This was accomplished by repeating all scans on an empty sample container. In the present work we adopted a different approach to measure both components. With the sample in place, background scans were collected at wave vectors far from the 1D AF zone center, at $l = 1.2$ or $l = 0.8$. Due to the very steep dispersion of magnetic excitations along the chain axis, no magnetic signal is expected at these positions in the energy range covered in our experiments. In all cases the background signal was measured at both field values H_1 and H_2, but was found to be field independent, as expected.

The main assumption behind the ''spin-flop'' polarization analysis is that the magnetic field needed to induce the transition is weak on the energy scale set by the strength of relevant interchain interactions, the experimental energy range, and the energy resolution of the spectrometer. In other words, in Eq. (1), it is only the angle $\alpha_{\mathbf{q}}$ that changes on going through the spin-flop transition, while the structure factors $S^{\perp}(\mathbf{q},\omega)$ remain unaffected. The validity of this assumption for the type of measurements performed in this work was argued in detail in Ref. 6.

III. EXPERIMENTAL RESULTS

Typical raw data sets measured in constant-Q and constant-E modes at $T = 1.5$ K are shown in Fig. 1. At energies in excess of about 2Δ the scattering is practically unaffected by the phase transition [Fig. 1(b)]. The contrast in inelastic intensity measured at two different field values is most apparent at energy transfers of about Δ [Figs. 1(a) and 1(c)]. Separating the longitudinal and transverse contributions as described in the previous section yields the constant-Q scans shown in Figs. 2–4. The evolution of the instrumental full width at half maximum (FWHM) resolution ellipsoid in the course of each scan is shown in the right part of each figure. Typical constant-E data are shown in Fig. 5. A contour and false color plot based on a series of ten such scans taken with a 1-meV energy step is shown in Fig. 6.

Certain important features of the measured transverse and

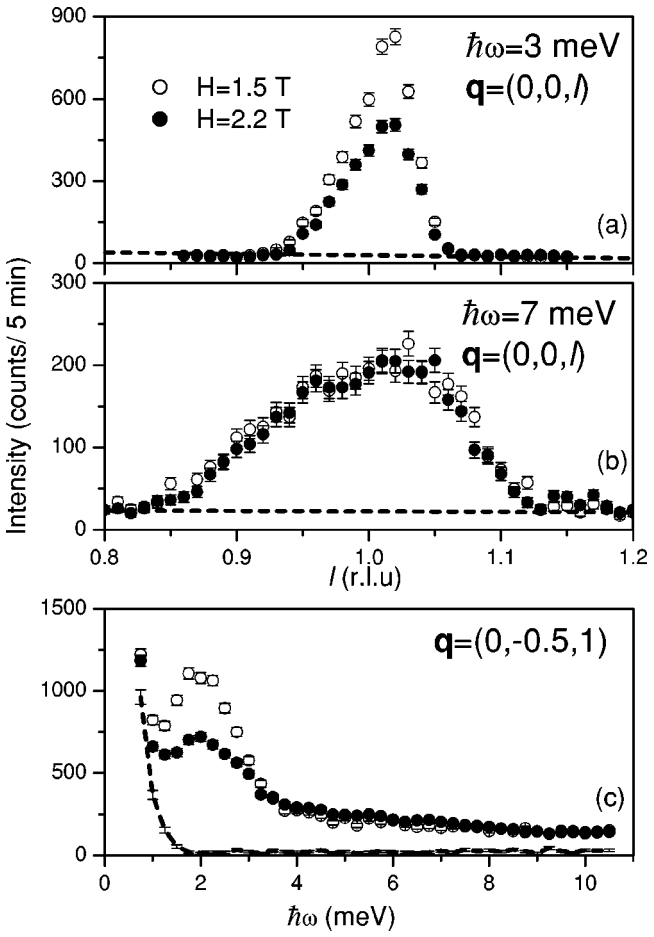

FIG. 1. Typical constant-E scans (a) and (b) and constant-Q scans (c) measured in $BaCu_2Si_2O_7$ in magnetic fields $H=1.5$ T (open circles) and $H=2.2$ T (solid circles) applied along the crystallographic c axis. The dashed lines in (a) and (b) represent the background obtained by linear interpolation between intensities measured at $l=0.8$ and $l=1.2$. In (c) the dashed line is the background scan measured at $\mathbf{q}=(0, -0.5, 1.2)$.

longitudinal dynamic structure factors can be identified even without a quantitative data analysis. An important experimental observation is that longitudinal excitations show a steep dispersion along the chains. As can be seen in Fig. 6, the corresponding spin velocity is the same as for transverse-polarized spin waves. Furthermore, at high-energy transfers (above ≈ 7 meV) the scattering is almost *polarization independent* to within experimental accuracy and resolution (Figs. 2–5). Such behavior is consistent with our general expectation that interchain interactions become almost irrelevant at energies well above the gap energy Δ. The dynamic structure factor in this regime is as in isolated chains, and is therefore almost isotropic.

At smaller energy transfers the structure factors for longitudinal and transverse polarizations are noticeably different. As observed in previous detailed studies,[8] transverse-polarization constant-Q scans are characterized by a sharp spin-wave peak, whose position and intensity is strongly dependent on momentum transfer $\mathbf{q}_\perp$ in the direction perpendicular to the spin chains. The effect of this pronounced dispersion can be seen in Figs. 2(a)–4(a). In contrast, longitudinal-polarized scans lack the sharp component and are *almost independent of* $\mathbf{q}_\perp$ [Figs. 2(b)–4(b)]. Such behavior is reminiscent of that for the transverse-polarized *continuum* that also shows very little variation with $\mathbf{q}_\perp$.[8]

IV. THEORY

Before discussing the quantitative analysis of the experimental data we shall describe the application of the chain-MF/RPA approach to the problem of weakly coupled chains in $BaCu_2Si_2O_7$.

A. Hamiltonian and definitions

Following Refs. 13 and 8 the spin Hamiltonian for $BaCu_2Si_2O_7$ is written as

$$H = H_{\text{chains}} + H',$$

$$H_{\text{chains}} = J \sum_{i,j,n} \mathbf{S}_{i,j,n} \cdot \mathbf{S}_{i,j,n+1},$$

$$H' = \sum_{i,j,n} J_x \mathbf{S}_{i,j,n} \cdot \mathbf{S}_{i+1,j,n} + J_y \mathbf{S}_{i,j,n} \cdot \mathbf{S}_{i,j+1,n} + J_3 \mathbf{S}_{i,j,n} \cdot (\mathbf{S}_{i+1,j+1,n} + \mathbf{S}_{i+1,j-1,n}). \quad (2)$$

The Fourier transform of the interchain coupling is defined as

$$J'(\mathbf{q}) = J_x \cos(q_x) + J_y \cos(q_y) + J_3[\cos(q_x + q_y) + \cos(q_x - q_y)]. \quad (3)$$

In order to comply with the formalism of Refs. 5 and 3 it is convenient to introduce new spin variables $\tilde{S}^\alpha$:

$$S^x_{i,j,n} = \tilde{S}^x_{i,j,n}, \quad S^\alpha_{i,j,n} = (-1)^j \tilde{S}^\alpha_{i,j,n}, \quad \alpha = y,z. \quad (4)$$

The transformation (4) leaves H_{chains} invariant, but flips the signs of J_y and J_3 in the interaction of the y and z components of the spin operators in H'. The staggered magnetization at $T=0$ is defined as

$$\langle \tilde{S}^\alpha_{i,j,n} \rangle = \delta_{\alpha,z} (-1)^n m_0. \quad (5)$$

B. Chain-MF and field-theoretical results for a single chain

The first step in the chain-MF/RPA is a mean-field decoupling of the interchain interaction H':[4]

$$\tilde{S}^\alpha_{i,j,n} = \langle \tilde{S}^\alpha_{i,j,n} \rangle + \delta \tilde{S}^\alpha_{i,j,n}, \quad (6)$$

where $\delta \tilde{S}^\alpha_{i,j,n}$ denote (small) fluctuations around the expectation value. Substituting Eq. (6) in H' we obtain a mean-field Hamiltonian

$$H_{\text{MF}} = \sum_{i,j} \sum_n J \tilde{\mathbf{S}}_{i,j,n} \cdot \tilde{\mathbf{S}}_{i,j,n+1} + h(-1)^n \tilde{S}^z_{i,j,n},$$

$$h = 2(J_x - J_y - 2J_3) m_0 \equiv J' m_0. \quad (7)$$

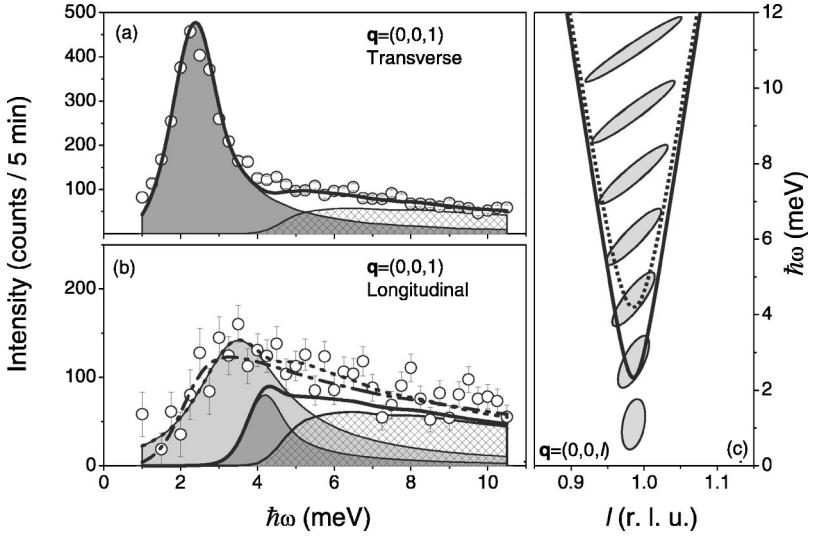

FIG. 2. Transverse (a) and longitudinal (b) components of a constant-Q scan measured in $BaCu_2Si_2O_7$ at $\mathbf{q}=(0,0,1)$. In (a) the heavy solid line is a fit using an empirical-model cross that includes a sharp single-mode contribution (gray area) and a "truncated Müller-ansatz" (TMA) continuum part (hatched area). Two such fits are shown in (b) as a heavy solid line and a dotted line. For both, the hatched area represents the TMA continuum. The dark shaded area is the single-mode longitudinal component as predicted by chain-MF/RPA theory. The light shaded area is the same component that was allowed to have a nonzero adjustable intrinsic width and adjustable intensity. Finally, the dash-dotted line is a fit based on the TMA alone, with no single-mode contribution. For more details see text. The shape of the scans is influenced by the evolution of the spectrometer resolution function in the course of the scan (c).

The Hamiltonian (7) describes an ensemble of *uncoupled* spin-$\frac{1}{2}$ Heisenberg chains in a staggered magnetic field,

$$H_{1D}=\sum_n J\tilde{\mathbf{S}}_n\cdot\tilde{\mathbf{S}}_n+h(-1)^n\tilde{S}^z_{n+1}. \tag{8}$$

The next step is to find a solution for an isolated chain in an external field h. Since in the limit of weak interchain coupling the latter is expected to be small compared to J, it is possible to determine dynamical correlation functions at low energies $\hbar\omega\ll J$ by means of field-theory methods. A standard bosonization analysis gives the following scaling limit of Eq. (8):

$$\mathcal{H}_{1D}=\int dx\left[\frac{v}{2}(\partial_x\phi)^2+\frac{1}{2v}(\partial_t\phi)^2+Ch\cos(\sqrt{2\pi}\phi)\right]. \tag{9}$$

In this formula $v=\pi Ja_0/2$ is the spin velocity of the spin-$\frac{1}{2}$ Heisenberg chain[15] and C is a nonuniversal constant that was calculated in Ref. 16. The model (9) is known as the quantum sine-Gordon model (SGM) and is exactly solvable. The spectrum is formed by scattering states of four particles, called soliton s, antisoliton $\bar{s}$, breather B_1, and breather B_2. The breathers themselves are soliton-antisoliton bound states. All four particles have gapped relativistic dispersion relations:[17]

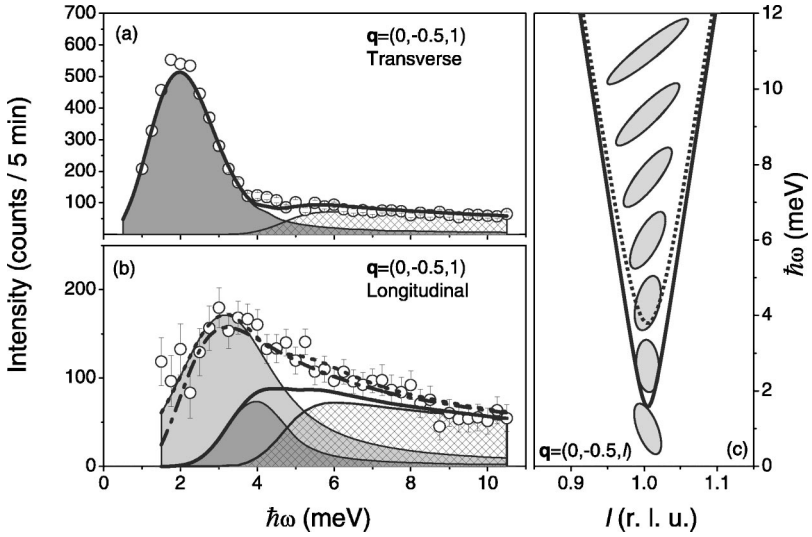

FIG. 3. Transverse (a) and longitudinal (b) components of a constant-Q scan measured in $BaCu_2Si_2O_7$ at $\mathbf{q}=(0,-0.5,1)$. Lines and the plot shown in (c) are the same as in Fig. 2.

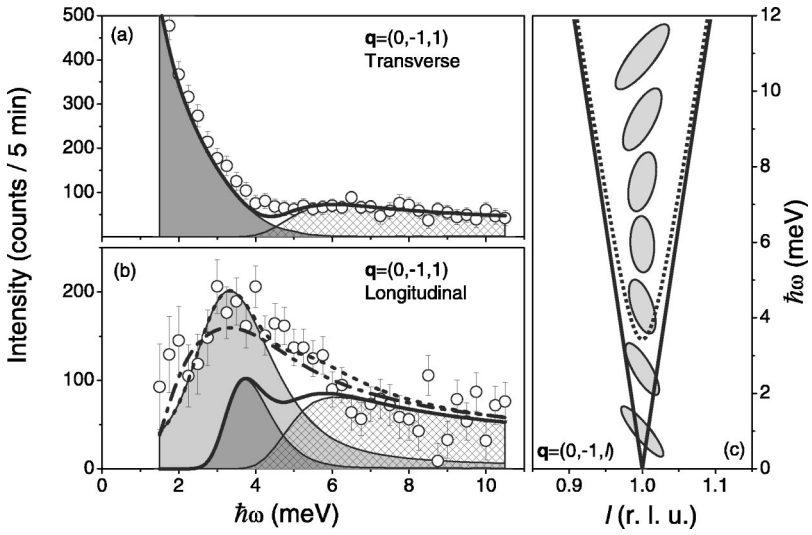

FIG. 4. Transverse (a) and longitudinal (b) components of a constant-Q scan measured in $BaCu_2Si_2O_7$ at $\mathbf{q}=(0,-1,1)$. Lines and the plot shown in (c) are the same as in Fig. 2.

$$E_\alpha=\Delta\cosh\theta,\quad P_\alpha=\frac{\Delta}{v}\sinh\theta,\quad \alpha=s,\ \bar{s},\ B_1,$$

$$E_{B_2}=\sqrt{3}\Delta\cosh\theta,\quad P_{B_2}=\frac{\sqrt{3}\Delta}{v}\sinh\theta. \tag{10}$$

Using the integrability of the SGM it is possible to determine correlation functions by exact methods. As described in Ref. 18, the expectation value of the staggered magnetization can be calculated from the results of Ref. 16:

$$m_0=C\langle\cos\sqrt{2\pi}\phi\rangle\approx c\left(\frac{h}{J}\right)^{1/3}\left[\ln\left(\frac{J}{h}\right)\right]^{1/3},$$

$$c=\frac{2^{2/3}}{3\sqrt{3}\pi}\left[\frac{\Gamma(\frac{3}{4})}{\Gamma(\frac{1}{4})}\right]^{4/3}\left[\frac{\Gamma(\frac{1}{6})}{\Gamma(\frac{2}{3})}\right]^2. \tag{11}$$

Equation (11) is the self-consistency equation of the MF approximation (recall that $h=m_0J'$) and is easily solved for m_0:

$$m_0\approx A_1\left[\frac{J'}{J}\ln\left(\frac{2.584\,95J}{J'}\right)\right]^{1/2},$$

$$A_1=\frac{\sqrt{2}}{3^{7/4}\pi^{3/2}}\left[\frac{\Gamma(\frac{3}{4})}{\Gamma(\frac{1}{4})}\right]^2\left[\frac{\Gamma(\frac{1}{6})}{\Gamma(\frac{2}{3})}\right]^3\approx 0.294\,691. \tag{12}$$

We note that the constant 2.584 95 should not be taken seriously since we have ignored subleading logarithmic corrections. The result (12) is found to be in good agreement (for small J'/J) with a phenomenological expression obtained from quantum Monte Carlo simulations in Ref. 19. The soliton gap as a function of the staggered field h has been calculated in Refs. 20 and 18. Expressing h in terms of m_0 by Eq. (7) and then using Eq. (12) we obtain

$$\frac{\Delta}{J}\approx A_2\frac{J'}{J}\left[\ln\left(\frac{2.584\,95J}{J'}\right)\right]^{1/2},$$

$$A_2=\frac{1}{3\pi}\left[\frac{\Gamma(\frac{3}{4})}{\Gamma(\frac{1}{4})}\right]^2\left[\frac{\Gamma(\frac{1}{6})}{\Gamma(\frac{2}{3})}\right]^3\approx 0.841\,916. \tag{13}$$

Note that this result is at variance with that of Ref. 5, where it was reported that (in our notations)

$$\Delta\approx\frac{6.175}{4}J'=1.544J'. \tag{14}$$

The polarization-dependent dynamic structure factors of interest to us in the present study are directly related, through the fluctuation-dissipation theorem, to the imaginary parts of the corresponding dynamic susceptibilities. For a single spin chain in a self-consistent staggered mean field the latter were derived in Ref. 3, and are expressed in terms of a spectral sum over intermediate states with one, two, three, etc. particles. In the energy range in which we are interested here ($\hbar\omega\lesssim 5\Delta$), the contributions due to intermediate states with three or more particles are negligible. With all contributions from intermediate states with at most two particles taken into account, the expressions for the dynamic susceptibilities are

$$\tilde{\chi}^{\perp}_{1\mathrm{D}}(\omega,\pi+q)=\frac{2|F_1|^2}{\Delta^2-s^2-i\epsilon}-\int_0^\infty\frac{d\theta}{\pi}\frac{2|F^{\cos}_{+-}(\theta)|^2+|F^{\cos}_{11}(\theta)|^2}{s^2-[2\Delta\cosh(\theta/2)]^2+i\epsilon}-\int_0^\infty\frac{d\theta}{\pi}\frac{|F^{\cos}_{22}(\theta)|^2}{s^2-[\sqrt{12}\Delta\cosh(\theta/2)]^2+i\epsilon}, \tag{15}$$

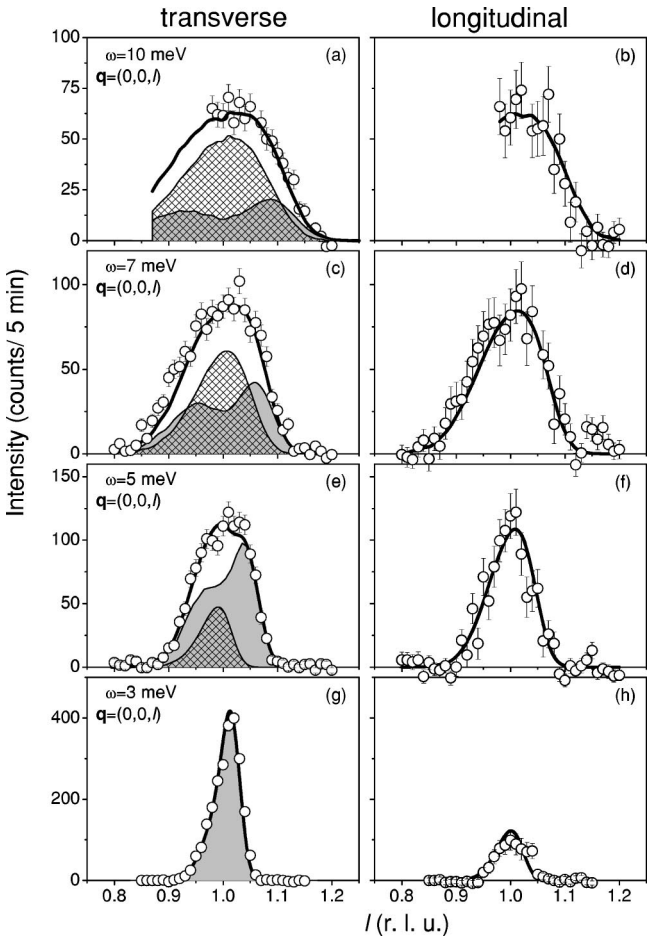

FIG. 5. Transverse (a), (c), (e), and (g) and longitudinal (b), (d), (f), and (h) components of typical constant-E scans measured in $BaCu_2Si_2O_7$ along the $\mathbf{q}=(0,0,l)$ direction. Lines are fits to the experimental data as described in the text.

$$\tilde{\chi}^{\parallel}_{1D}(\omega,\pi+q)=\frac{2|F_2|^2}{3\Delta^2-s^2-i\epsilon}-\int_0^{\infty}\frac{d\theta}{\pi}\frac{2|F^{\sin}_{+-}(\theta)|^2}{s^2-[2\Delta\cosh(\theta/2)]^2+i\epsilon}-\int_0^{\infty}\frac{d\theta}{\pi}\frac{2|F^{\sin}_{12}(\theta)|^2}{s^2-4\Delta^2\left(1+\frac{\sqrt{3}}{2}\cosh\theta\right)+i\epsilon}. \quad (16)$$

Here $s^2=\hbar^2\omega^2-v^2q^2/a_0^2$ and the functions $F^{\sin}_{\epsilon_1\epsilon_2}(\theta)$, $F^{\cos}_{\epsilon_1\epsilon_2}(\theta)$ are determined in Ref. 3 *up to an overall constant factor* denoted by Z. Analytic expressions for the constants $|F_{1,2}|^2$ are also given in Ref. 3 and have the numerical values

$$|F_1|^2\simeq 0.0533Z, \quad |F_2|^2\simeq 0.0262Z. \quad (17)$$

Using recent theoretical advances[16,18] it is possible to calculate the normalization Z with good accuracy although we do not need it in the present calculation (see below). Note that

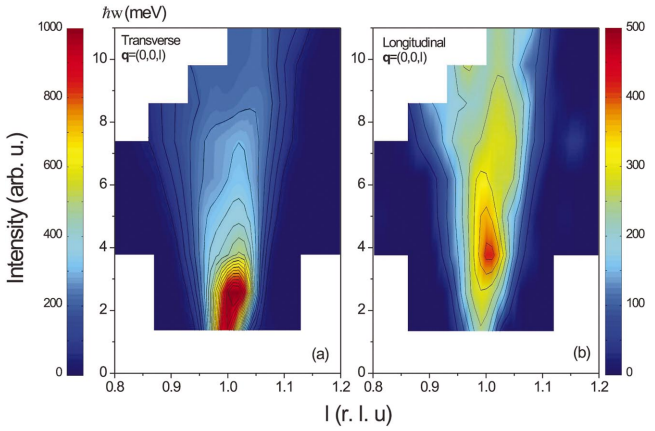

FIG. 6. (Color) Contour and false-color plot of the transverse-polarized (left) and longitudinal-polarized (right) inelastic scattering measured in $BaCu_2Si_2O_7$ near the 1D AF zone center $(0,0,1)$.

both the longitudinal and transverse dynamic susceptibilities feature single-mode and continuum contributions. In the transverse-polarization channel the single-mode (SM) excitations have the energy Δ, while the energy of the longitudinal mode is $\sqrt{3}\Delta$. Regardless of polarization, the continuum has a gap of 2Δ. While the transverse continuum is singular on its lower bound, the one in the longitudinal polarization channel is not.

C. Coupled chains and the RPA

In the final stage of the described approach the dynamic susceptibilities of *coupled* chains (in the original spin variables) are expressed as

$$\chi^{\alpha}_{3D}(\omega,\mathbf{q})=\frac{\tilde{\chi}^{\alpha}_{1D}(\omega,q_{\parallel})}{1-J'(\mathbf{q})[\tilde{\chi}^{\alpha}_{1D}(\omega,q_{\parallel})+\Sigma^{\alpha}(\omega,\mathbf{q})]}, \quad (18)$$

where $\alpha=\perp,\parallel$. In Eq. (18) $\Sigma^{\perp}$ and $\Sigma^{\parallel}$ are the self-energies that are expressed in terms of integrals involving three-point, four-point, etc. correlation functions of spin operators. The analogous expressions in the disordered phase were derived in Refs. 21–23. To date, the relevant multipoint correlation function has not been calculated for the sine-Gordon model. The essence of the RPA is to simply neglect the self-energies.[4,5] In other words, one sets

$$\Sigma^{\perp}=\Sigma^{\parallel}=0. \quad (19)$$

One problem is that in this approximation the transverse susceptibility will not have a zero-frequency spin-wave pole at the 3D magnetic zone center, as it should, spin waves being the Goldstone modes of the magnetically ordered state. In order for the pole to be exactly at $\omega=0$ the full self-energy Σ^{xx} must, in fact, be included. A work-around was suggested by Schulz.[5] Assuming the RPA is a reasonably good approximation, the pole in $\chi^{\perp}_{3D}(\omega,0,\pi,\pi)$ will occur at a very small frequency. As a result,

$$1\approx J'(0,\pi)\tilde{\chi}^{\perp}_{1D}(0,\pi). \quad (20)$$

The idea is to replace pole 1 by an equality

$$1 = J'(0,\pi)\tilde{\chi}^{\perp}_{1D}(0,\pi), \tag{21}$$

and then use pole 2 to fix the overall normalization of $\tilde{\chi}^{\perp}_{1D}(\omega,q)$. Following this logic, we may carry out the integral in chixx numerically to obtain

$$Z \approx 7.994 \frac{M^2}{J'(0,\pi)}. \tag{22}$$

Now it is a simple matter to determine $\chi^{\alpha}_{3D}(\omega,\mathbf{k},q)$ by evaluating the 1D susceptibilities numerically and then inserting them into the RPA.

As explained in Ref. 3, the resulting dynamic susceptibility for transverse spin fluctuations in coupled chains contains a pair of spin-wave excitations that disperse perpendicular to the spin chains, and are, by design, gapless. The longitudinal mode also disperses in the direction perpendicular to the chains, but retains a nonzero gap at the 3D magnetic zone center. Under the approximations made, the lower bounds of the continua remain at 2Δ and are independent of $\mathbf{q}_{\perp}$, regardless of polarization. The singularity at the lower bound of the transverse-polarized continuum vanishes and persists only at the ''magic'' wave vector $\mathbf{q}_0$, such that $J'(\mathbf{q}_0) \equiv 0$. For $BaCu_2Si_2O_7$ $\mathbf{q}_0 = (0.5, 0.5, 1)$. At $\mathbf{q}_0$ the dynamic structure factor is as for uncoupled chains in a staggered field and the gap Δ can be observed directly.

D. Results for $BaCu_2Si_2O_7$

The exchange parameters J, J_x, J_y, and J_3 for $BaCu_2Si_2O_7$ are known with very good accuracy from the previously measured spin-wave dispersion relation.[8] Using these numerical values the low-energy part of transverse and longitudinal structure factors were calculated for several wave vectors on the $(0, k, 1)$ reciprocal-space rods using the chain-MF/RPA described above. The results are visualized in Fig. 7. To improve the visual effect, any singularities in these plots were eliminated by convoluting the calculated profiles with a Gaussian kernel of a fixed FWHM of 0.2 meV. Note that this width is still considerably narrower than the typical resolution of a three-axis instrument in our experiments. A comparison of these calculation results to actual neutron-scattering data is the subject of the next section.

V. ANALYSIS OF EXPERIMENTAL DATA

To better understand the experimental results and perform a quantitative comparison between measured and calculated dynamic structure factors one has to take into account the effects of experimental resolution. This is best done by fitting the data to a parametrized model cross-section function numerically convoluted with the four-dimensional resolution function of the instrument.

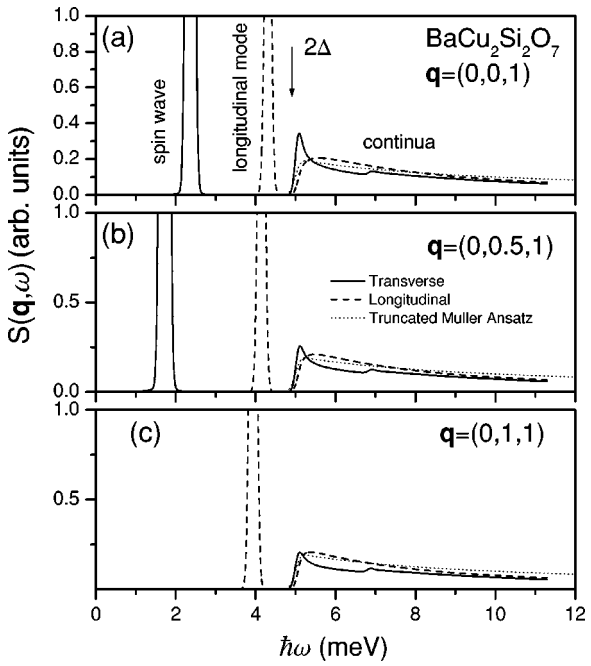

FIG. 7. Longitudinal (dashed lines) and transverse (solid lines) dynamic structure factors of $BaCu_2Si_2O_7$ at several wave vectors, calculated within the chain-MF/RPA. The calculated structure factors were regularized by convolution with a Gaussian function of 0.2-meV FWHM. The dotted line shows the fit function used in the analysis of neutron-scattering data.

A. A model cross section

In Ref. 8 for this purpose we have successfully employed a model cross section designed to reproduce the main features of the chain-MF/RPA calculations. The first component of the fit function for transverse excitations represents the long-lived spin waves and is written exactly as in chain-MF/RPA theory:

$$S^{\perp}_{SM}(\mathbf{q},\omega) = A \frac{[1-\cos(\pi l)]}{2\omega_{\perp}(\mathbf{q})} \times \{\delta[\omega - \omega_{\perp}(\mathbf{q})] + \delta[\omega + \omega_{\perp}(\mathbf{q})]\}. \tag{23}$$

Here $\omega^2_{\perp}(\mathbf{q})$ is the spin-wave dispersion relation given by

$$\omega^2_{\perp}(\mathbf{q}) = \frac{\pi^2}{4} J^2 \sin^2(\pi l) + \frac{\Delta^2}{|J'|}[|J'| + 2J'(\mathbf{q})], \tag{24}$$

where $J'(\mathbf{q})$ is defined by Eq. (3).

The second component of the fit function for transverse excitations approximates the continuum. We have previously found that, at least for wave vectors on the $(0, k, 1)$ reciprocal-space rod, continuum scattering can be very well approximated by the ''truncated Müller-ansatz'' (TMA) function:[24]

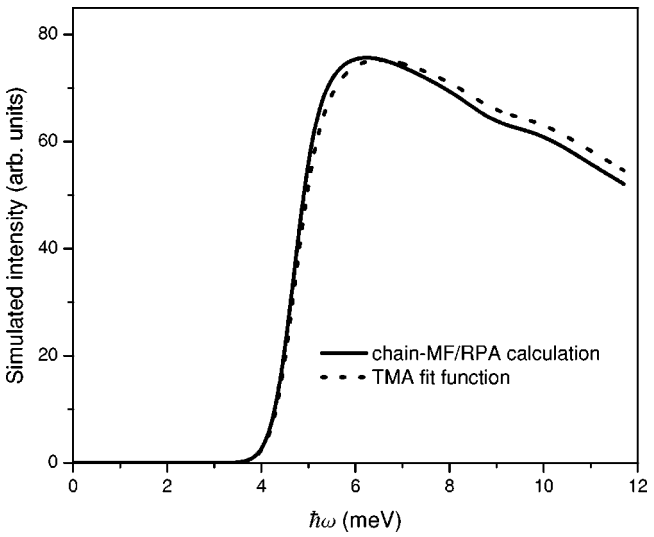

FIG. 8. Comparison of simulated scans across the transverse-polarized continuum at $\mathbf{q}=(0, 0, 1)$ based on the exact chain-MF/RPA result (solid line) and the empirical TMA fitting function that was used to analyze the neutron-scattering data (dotted line). Given the effects of experimental resolution that were taken into account in these simulations, the two curves are virtually identical.

$$S_c^{\perp}(\mathbf{q},\omega)=\frac{\alpha A}{2}\frac{[1-\cos(\pi l)]}{\sqrt{\omega^2-\frac{\pi^2}{4}J^2\sin^2(q_{\|})}}\times\theta\left[\omega^2-\Delta_{c,\perp}^2-\frac{\pi^2}{4}J^2\sin^2(\pi l)\right]. \quad (25)$$

The TMA is plotted in thin dotted lines in Figs. 7(a)–7(c) for a direct comparison to our chain-MF/RPA result. Conveniently, given the experimental resolution width, the two functional forms are almost indistinguishable. This fact is illustrated in Fig. 8, which shows the transverse continuum obtained in the actual chain-MF/RPA calculation for $\mathbf{q}=(0, 0, 1)$ (solid line), along with the form 25 (dotted line), both profiles being numerically convoluted with the resolution function of the instrument. Resolution effects taken into account, an almost perfect match between the chain-MF/RPA calculation for $BaCu_2Si_2O_7$ and Eqs. (23) and (25) can be obtained for the entire range of energy and momentum transfers covered in our experiments by choosing $\Delta_{c,\perp}=5.0$ meV and $\alpha=0.17$ meV^{-1}.

Just like the transverse-polarized part, the fit function for longitudinal scattering is composed of a single-mode and continuum components. The dispersion relation and dynamic structure factor for the single-mode contribution are written as

$$S_{\mathrm{SM}}^{\|}(\mathbf{q},\omega)=\frac{\gamma}{2}A\frac{[1-\cos(\pi l)]}{2\omega_{\|}(\mathbf{q})}\frac{\Gamma/\pi}{[\omega-\omega_{\|}(\mathbf{q})]^2+\Gamma^2}, \quad (26)$$

$$\omega_{\|}^2(\mathbf{q})=\frac{\pi^2}{4}J^2\sin^2(\pi l)+\Delta_{\|}^2+\frac{\Delta^2 J'(\mathbf{q})}{|J'|}. \quad (27)$$

These equations are a generalization of Eqs. (12) and (13) in Ref. 8, that allow for a damping of the longitudinal mode. The adjustable parameter $\Delta_{\|}$ is the energy of the longitudinal mode at the RPA "magic" point. The coefficient γ is an adjustable parameter that determines the intensity ratio of longitudinal and transverse excitations, while A is an overall intensity prefactor used for both polarizations [see Eqs. (4), (5), and (10) in Ref. 8]. In Eq. (26) the δ function is replaced (for positive energy transfers) by a Lorentzian profile with a half width at half height of Γ.

The longitudinal-polarized excitation continuum was modeled using the same truncated Müller-ansatz cross-section function as previously done for the transverse case:

$$S_c^{\|}(\mathbf{q},\omega)=\frac{\beta A}{2}\frac{[1-\cos(\pi l)]}{\sqrt{\omega^2-\frac{\pi^2}{4}J^2\sin^2(q_{\|})}}\times\theta\left[\omega^2-\Delta_{c,\|}^2-\frac{\pi^2}{4}J^2\sin^2(\pi l)\right]. \quad (28)$$

Note that, unlike in Ref. 8, we use separate relative intensity prefactors and (pseudo)gap energies for the transverse and longitudinal continua. By choosing $\Delta_{c,\|}=\Delta_{c,\perp}$ and $\beta=\alpha$ one can accurately reproduce the chain-MF/RPA result for $BaCu_2Si_2O_7$ to within resolution effects in the energy and momentum-transfer ranges covered in the present study.

B. Transverse polarization

As a first step in the quantitative data analysis, the two-component model cross section for transverse polarization was numerically convoluted with the calculated spectrometer resolution function and fit to the transverse components of all scans measured in this work (429 total scan points). The relevant parameters of the model, including the mass gap $\Delta=2.51(2)$ meV; the interchain exchange constants $J_x=-0.460(7)$ meV, $J_y=0.200(6)$ meV, and $2J_3=0.152(7)$ meV; the in-chain exchange parameter $J=24.1$ meV; the continuum gap $\Delta_{c,\perp}=4.8(2)$ meV; and the ratio $\alpha=0.20(3)$ meV^{-1} of single-mode and continuum intensities, were determined previously with very good accuracy.[13,8] When analyzing the present data, only the overall scaling factor was treated as an adjustable parameter. A good ($\chi^2=2.7$) one-parameter *global* fit to all the measured scans was obtained (heavy solid lines in Figs. 2(a)–4(a) and Figs. 5(a)–5(g). The hatched and gray areas of Figs. 2 –5 represent the continuum and single-mode components, respectively.

As mentioned in the previous section, our chain-MF/RPA theoretical result for $BaCu_2Si_2O_7$ corresponds to fitting function parameters $\Delta_{c,\perp}=2\Delta=5.0$ meV and $\alpha=0.17$ meV^{-1}, which is in remarkably good agreement with previous and current experiments. We conclude that for transverse polarization the chain-MF/RPA not only predicts the correct spin-wave dispersion relation and continuum gap energy, but provides an accurate estimate for the *intensity* of the lower-energy part of the continuum.

C. Longitudinal polarization

The agreement with theory is not nearly as good in the longitudinal-polarization channel. In the chain-MF/RPA the LM is infinitely sharp and corresponds to $\Gamma \rightarrow 0$ in Eq. (26). The LM's energy and intensity are given by $\Delta_{\parallel} = \sqrt{3}\Delta$, and $\gamma \approx 0.49$. Our chain-MF/RPA calculation for the longitudinal continuum in $BaCu_2Si_2O_7$ is very well approximated by Eq. (28) with $\Delta_{c,\perp} = \Delta_{c,\parallel}$ and $\beta = \alpha$. Using these values in the model cross section convoluted with the resolution function of the spectrometer, we can simulate the measured scans as expected in the chain-MF/RPA model. These simulations are shown in solid lines in Figs. 2(b)–4(b). The dark gray area represents the longitudinal mode, and the hatched area is the continuum contribution. It is clear that at all values of $\mathbf{q}_{\perp}$ the model fails to reproduce the observed longitudinal spectrum. The discrepancy is greatest at energy transfers *below* 2Δ, where the chain-MF/RPA model predicts no scattering except that by the LM. At higher-energy transfers the agreement between theory and experiment becomes progressively better.

Of course, much better fits to the experimental data can be obtained if the central energy $\Delta_{\parallel}$, intensity prefactor γ, and intrinsic energy width Γ of the longitudinal mode are allowed to vary. The result of fitting this ''damped LM'' model globally to the entire data set for longitudinal polarization (358 data) is shown in Figs. 2(b)–4(b) as dotted lines, and corresponds to $\chi^2 = 1.5$. The fit yields $\Delta_{\parallel} = 2.1(1)$ meV, $\gamma = 1.2(2)$, and $\Gamma = 1.5(2)$ meV. This analysis confirms the main conclusion of the preliminary study of Ref. 6: to adequately describe the longitudinal scattering in $BaCu_2Si_2O_7$ in terms of a ''longitudinal mode'' one has to assume a substantial intrinsic width, comparable to the mode's central energy and to its separation from the continuum threshold. The ''longitudinal mode'' can therefore be no longer considered a separate feature, since it is merged with the strong continuum at higher-energy transfers. The energy separation of single-mode and continuum excitations previously observed for transverse polarization is *absent* in the longitudinal channel. It is important to emphasize that the mismatch between theory and experiment involves more than simply a broadening of the LM. Experimentally one observed considerably more scattering below 2Δ energy transfer than the LM could provide in the chain-MF/RPA model. As a result, the refined value of γ is almost four times larger than expected, and the ''LM'' is almost equal in intensity to a transverse spin wave.

The measured data can, in fact, be reproduced without including a single-mode longitudinal component in the cross section. This ''continuum-only'' model corresponds to $\gamma = 0$, while $\Delta_{c,\parallel}$ and $\alpha_{\parallel}$ are the adjustable parameters. Rather good global fits to 249 data points at $k = 0$ are obtained with $\Delta_{c,\parallel} = 2.0(1)$ meV, $\alpha_{\parallel} = 0.22(0.01)$, and $\chi^2 = 1.16$. Scan simulations based on these parameter values are plotted by heavy solid lines in Figs. 5(b), 5(d), 5(f), and 5(h), and by a dash-dotted line in Fig. 2(b). The parameter $\Delta_{c,\parallel}$ was fit separately for the constant-Q scans at $k = -0.5$ and $k = -1$, yielding $\Delta_{c,\parallel} = 1.8(1)$ meV and $\Delta_{c,\parallel} = 1.5(1)$ meV, respectively. The results are shown in dash-dotted lines in Figs. 3(b) and 4(b). The variation of $\Delta_{c,\parallel}$ as a function of $\mathbf{q}_{\perp}$ corresponds to the dispersion of the longitudinal mode built into the ''damped LM'' model.

VI. CONCLUDING REMARKS

Based on the neutron-scattering results we can now provide a phenomenological description of the longitudinal excitations in weakly interacting quantum spin chains. There is no sharp longitudinal mode, but a broad asymmetric peak that is inseparable from the continuum at higher frequencies. This feature is practically independent of $\mathbf{q}_{\perp}$, but has a steep dispersion along the chain axis. The scattering starts at energies well below 2Δ, and its intensity at low energies is considerably greater than that predicted by the chain-MF/RPA.

It appears that the established chain-MF/RPA model is at the same time remarkably good in predicting the transverse correlations of weakly coupled chains, and vastly inadequate as far as longitudinal fluctuations are concerned. Admittedly, one can never entirely dismiss the possibility that the disagreement between theory and experiment in the latter case may, in fact, be due to some intrinsic flaw in the unconventional technique that we used for polarization analysis. However, having repeatedly scrutinized the measurement procedure, we were unable to identify any potential sources of systematic error that could account for the observed discrepancies with theoretical calculations. We thus conclude that the discrepancies stem from limitations of the theoretical method itself. Among the assumptions and approximations associated with the chain-MF/RPA approach, the most likely source of errors is the uncontrolled discarding of the self-energies in the RPA. The RPA, by definition, acts on bare (purely 1D) dynamic susceptibilities at *particular wave vectors*. It excludes interactions between particles, such as processes that involve a decay of a particle with momentum $\mathbf{q}$ into a pair of particles with momenta $\mathbf{q}_1 + \mathbf{q}_2 = \mathbf{q}$. The contributions of such processes to the susceptibility involve 1D correlation functions of three or more spin operators. For spin chains that are *intrinsically* gapped such processes are expected to be suppressed, in which case the RPA will be fully justified. We can expect the RPA to be an almost perfect description of weakly coupled ladders or Haldane spin chains. For weakly coupled $S = \frac{1}{2}$ chains, however, the mean-field gap Δ is itself determined by J'. As a result, the transverse spectrum in the RPA is gapless, regardless of J'/J. Hence a longitudinal excitation can always decay into a pair of transverse-polarized spin waves. The RPA fails by excluding this effect. Comparing the results of the present study to the ones reported in Ref. 1 for $KCuF_3$, the question arises as to why there is a longitudinal mode, albeit damped, in the latter material but not in $BaCu_2Si_2O_7$. The main difference between the two materials is the strength of the interchain coupling: in $BaCu_2Si_2O_7$ the ratio of the bandwidths perpendicular to the chains and along the chains is $2\Delta/\pi J \simeq 0.066$, whereas it is approximately 0.2 for $KCuF_3$. This may suggest that a sufficiently strong dispersion perpendicular to the chains is necessary in order to stabilize a damped longitudinal mode. It would be interesting to investigate this issue by determining the damping of the longitudinal mode in MF/RPA.

ACKNOWLEDGMENTS

Work at the University of Tokyo was supported in part by a Grant-in-Aid for the COE Research ''SCP coupled system'' of the Japanese Ministry of Education, Culture, Sports, Science, and Technology. Oak Ridge National Laboratory is managed by UT-Battelle, LLC for the U.S. Department of Energy under Contract No. DE-AC05-00OR22725. F.H.L.E. was supported by the DOE under Contract No. DE-AC02-98 CH 10886. We would like to thank S. Maslov, I. Zaliznyak, and A. Tsvelik for illuminating discussions.

*Email address: zheludevai@ornl.gov

†Present address: Condensed Matter Sciences Division, Oak Ridge National Laboratory, Oak Ridge, TN 37831-6393.

[1] B. Lake, D. A. Tennant, and S. E. Nagler, Phys. Rev. Lett. **85**, 832 (2000).

[2] The polarized-neutron study is by B. Lake, D. A. Tennant, and S. E. Nagler (unpublished).

[3] F. H. L. Essler, A. M. Tsvelik, and G. Delfino, Phys. Rev. B **56**, 11 001 (1997).

[4] D. J. Scalapino, Y. Imry, and P. Pincus, Phys. Rev. B **11**, 2042 (1975).

[5] H. J. Schulz, Phys. Rev. Lett. **77**, 2790 (1996).

[6] A. Zheludev, K. Kakurai, T. Masuda, K. Uchinokura, and K. Nakajima, Phys. Rev. Lett. **89**, 197205 (2002).

[7] A. Zheludev, M. Kenzelmann, S. Raymond, E. Ressouche, T. Masuda, K. Kakurai, S. Maslov, I. Tsukada, K. Uchinokura, and A. Wildes, Phys. Rev. Lett. **85**, 4799 (2001).

[8] A. Zheludev, M. Kenzelmann, S. Raymond, T. Masuda, K. Uchinokura, and S.-H. Lee, Phys. Rev. B **65**, 014402 (2001).

[9] I. Tsukada, Y. Sasago, K. Uchinokura, A. Zheludev, S. Maslov, G. Shirane, K. Kakurai, and E. Ressouche, Phys. Rev. B **60**, 6601 (1999).

[10] I. Tsukada, J. Takeya, T. Masuda, and K. Uchinokura, Phys. Rev. Lett. **87**, 127203 (2001).

[11] A. Zheludev, E. Ressouche, I. Tsukada, T. Masuda, and K. Uchinokura, Phys. Rev. B **65**, 174416 (2002).

[12] A. Zheludev, M. Kenzelmann, S. Raymond, E. Ressouche, T. Masuda, K. Kakurai, S. Maslov, I. Tsukada, K. Uchinokura, and A. Wildes, Phys. Rev. Lett. **85**, 4799 (2000).

[13] M. Kenzelmann, A. Zheludev, S. Raymond, E. Ressouche, T. Masuda, P. Böni, K. Kakurai, I. Tsukada, K. Uchinokura, and R. Coldea, Phys. Rev. Lett. **64**, 054422 (2001).

[14] In other words, only the first term in Eq. (3) of Ref. 8 is of any importance in the studied **q** range.

[15] a_0 is the period of the spin chains that is equal to $c/2$ for $BaCu_2Si_2O_7$.

[16] S. Lukyanov and A. B. Zamolodchikov, Nucl. Phys. B **493**, 571 (1997).

[17] In Ref. 3 the mass gap Δ is denoted as M.

[18] I. Affleck and M. Oshikawa, Phys. Rev. B **60**, 1038 (1999).

[19] A. W. Sandvik, Phys. Rev. Lett. **83**, 3069 (1999).

[20] F. H. L. Essler, Phys. Rev. B **59**, 14 376 (1999).

[21] M. Bocquet, Phys. Rev. B **65**, 184415 (2002).

[22] V. Y. Irkhin and A. A. Katanin, Phys. Rev. B **61**, 6757 (2000).

[23] M. Bocquet, F. H. L. Essler, A. Tsvelik, and A. Gogolin, Phys. Rev. B **64**, 094425 (2001).

[24] In Ref. 8 there is a a factor-of-2 mistake in the quoted value of α. Note also that α is measured in reciprocal energy units.